

# SHEAR RESPONSE OF ISOLATED ANGLE BRACKETS FOR CROSS-LAMINATED TIMBER BUILDINGS

Boris AZINOVIĆ<sup>1</sup>, Miha KRAMAR<sup>2</sup>, Tomaž PAZLAR<sup>3</sup>, Meta KRŽAN<sup>4</sup>

#### **ABSTRACT**

In cross-laminated timber (CLT) buildings, acoustic behaviour presents a major concern due to low frequency noise transmission. To reduce the disturbing sound transmission over the flanking parts, special elastic layers with fine celled structure are being used between the CLT wall and CLT slab together with insulated angle bracket connections. However, the seismic response of the developed isolated connection and the influence of insulation bedding on the seismic response of CLT structures have not yet been studied.

In the paper, shear tests on small specimens of CLT panels placed on polyurethane elastomer insulation bedding and fastened to CLT floor with innovative insulated steel angle bracket are presented. Altogether 5 monotonic and 10 cyclic shear tests were performed. Specimens with four types of bedding material varying in stiffness and compression load were tested and compared with tests on specimens of panels and floors connected with uninsulated steel bracket without any bedding. The experiments have shown that insulation bedding does not have much influence on the load-bearing capacity and the ductility of the system; however insulation bedding changes the stiffness characteristics of the system which may be important when designing the structures.

Keywords: Sound-insulation bedding; insulated steel angle bracket; shear behaviour; experimental assessment; equivalent viscous damping

### 1 INTRODUCTION

In recent years several high-rise and complex apartment buildings have been built entirely by timber load-bearing elements, which was mainly achieved due to the development of cross laminated timber (CLT) structures (Abrahamsen and AS, 2017; Fragiacomo et al., 2011; Pei and van de Lindt, 2011; Reynolds et al., 2015). These structures have several advantages, such as: sustainability, energy efficiency, fast erection etc. However, other issues such as insufficient sound insulation, unpleasant vibration under serviceability loads and brittle behaviour of connections under severe seismic loads still need to be addressed.

One of the possibilities to reduce disturbing sound transmission over the flanking parts, which is more and more commonly used in CLT structures, is to use special elastic acoustic layers between the CLT wall and floor panels (Figure 1a). Depending on the design of the floor assembly, elastic layers can be placed underneath the wall or both underneath and on top of the walls. The selection of a suitable elastic layer depends on its resistance to static loads and on its dynamic parameters to provide a good acoustical

<sup>&</sup>lt;sup>1</sup>Researcher, Section for Timber Structures, The Slovenian National Building and Civil Engineering Institute, Ljubljana, boris.azinovic@zag.si

<sup>&</sup>lt;sup>2</sup>Researcher, Section for Timber Structures, The Slovenian National Building and Civil Engineering Institute, Ljubljana, miha.kramar@zag.si

<sup>&</sup>lt;sup>3</sup>Researcher, Section for Timber Structures, The Slovenian National Building and Civil Engineering Institute, Ljubljana, tomaz.pazlar@zag.si

<sup>&</sup>lt;sup>4</sup>Researcher, Section for Timber Structures, The Slovenian National Building and Civil Engineering Institute, Ljubljana, meta.krzan@zag.si

performance. Conventional connectors between CLT panels penetrate the elastic layer, create sound bridges and consequently reduce the acoustical performance. For this reason, special angle brackets have been developed by the Getzner and Pitzl companies where the rigid parts are elastically separated from each other (Figure 1b). These connectors are designed especially to withstand the horizontal loads, however, they are resistant also to tension, which is achieved by inclined fully-threaded screws inserted in the horizontal part of the angle bracket. The strength and stiffness of this innovative angle bracket in shear and tensile direction have therefore been increased via partially threaded screws used to connect the horizontal flange of the angle brackets to the floor panel and via special thick metal plate on top of the angle bracket. These types of connections should ensure high mechanical performance during earthquake which causes loads in shear and axial direction.

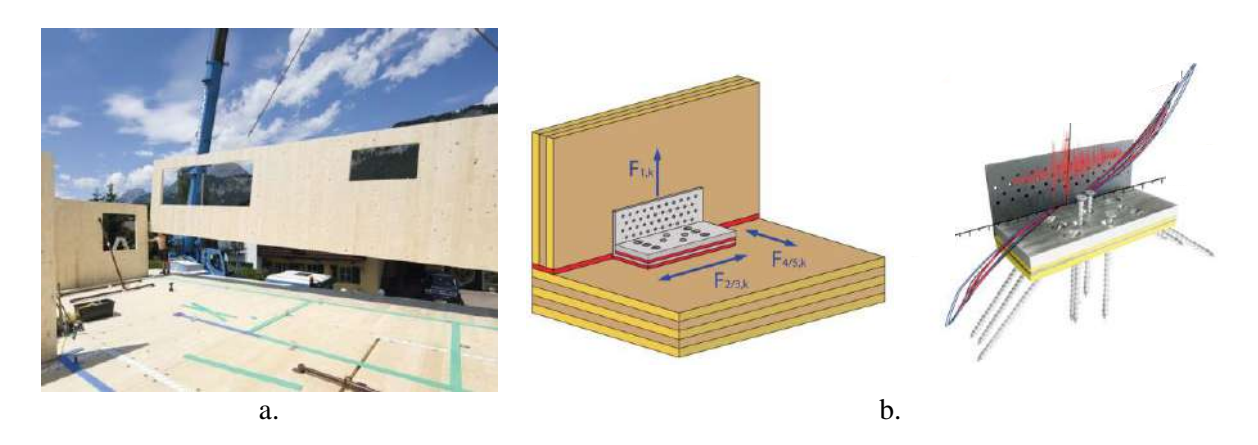


Figure 1. a. Elastic layers on CLT floor panels (Getzner, 2018) and b. Angle bracket concept GePi Pro (Pitzl and Getzner, 2018).

The objective of our research was to evaluate the mechanical properties, such as stiffness, strength and ductility, of insulated angle brackets which should be able to ensure high performance in shear and tension. In recent years, several studies have been conducted to better understand the mechanical behaviour of hold-downs and angle brackets by means of experimental and numerical tests in both monotonic and cyclic conditions (Benedetti et al., 2016; Casagrande et al., 2016; Giuseppe et al., 2018; Tomasi and Smith, 2015) and under combined shear and tensile loads (Liu and Lam, 2018). Regular angle brackets perform better under shear than under tensile loads (Flatscher et al., 2015; Gavrić et al., 2015). On the other hand, the hold-downs prove to have high stiffness and strength in tensile direction and very low stiffness and strength under shear actions (Benedetti et al., 2016). In the paper, the shear resistance of insulated angle brackets is investigated, while the tensile performance will be investigated in future studies.

The main aim of the paper is to show the resistance of the whole connection system composed of insulated angle bracket, elastic layer and surrounding timber. In order to investigate the behaviour of such connections developed for noise reduction, an experimental campaign including monotonic and cyclic shear tests on small specimens of CLT wall and floor panels connected via developed steel angle bracket was conducted. The behaviour of the steel angle brackets was tested and furthermore the influence of four type of insulation bedding materials varying in stiffness and their load capacity was studied.

# 2 EXPERIMENTS

#### 2.1 Specimens and material characterization

Specimens were designed considering limitations of the testing equipment. They were constructed from three-layer CLT panels with thickness 100 mm representing structural wall and five-layer CLT panels with thickness 140 mm representing structural floor (Figure 2). CLT panels were connected via 100x100x3 mm steel angle bracket (with length 240 mm) and fastened according to recommendations of the system provider. For mounting to floor, 10 partially threaded screws 8x160 mm were used; 4 were installed vertically in the

central part of the steel plate and next to them 3 were installed on each side at an angle 45° (as presented in Figure 1b). For fastening to the wall panel, 8 partially threaded screws 8x80 mm were used. The specimens varied in the grain orientation of the CLT wall panel; in some specimens the grain orientation of the outer layer was horizontal (i.e. parallel to floor panel), while for other the orientation was vertical (i.e. perpendicular to floor panel).

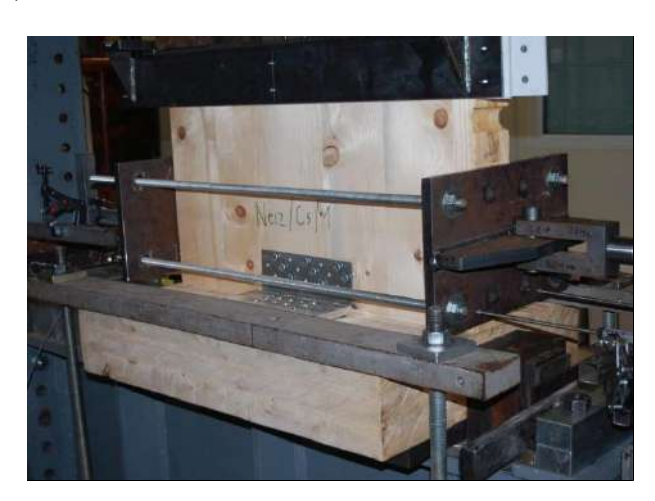


Figure 2. Test specimen - CLT wall and floor panel connected with angle bracket without insulation bedding

Between the wall and the floor panel, different bedding material of thickness 12.5 mm was laid. Two mixed cellular polyurethane sheets (sylomer®) and two closed cellular polyurethane sheets (sylodyn®) were used. Some characteristics of the bedding materials, provided by the manufacturer in their datasheets, are summarized in table 1.

Table 1. Insulation bedding material characteristics.

Material characteristics	SR 1200	SR 55	NF	NB
Static load limit* [MPa]	1.2	0.055	1.5	0.075
Approx. deflection at static load limit*	10 %	7 %	11 %	7 %
Operating load range* [MPa]	1.8	0.076	2.0	0.12
Approx. deflection at operating load range*	20 %	20 %	16 %	15 %
Load peaks* (short term, infrequent loads) [MPa]	6.0	2.0	8.0	2.0
Approx. deflection at load peaks*	35 %	75 %	50 %	70 %
Compression hardness [MPa]	1.08	0.061		

<sup>\*</sup> depending on the form factor; values apply to form factor 3

#### 2.2 Testing program, setup and protocol

Altogether 5 monotonic and 10 cyclic shear tests were conducted according to ISO 16670 (ISO, 2003) standard (Table 2). The tests were conducted in laboratory for structures at Slovenian National Building and Civil Engineering Institute (ZAG) in Ljubljana. In the test setup, the floor panel was completely fixed, while the out-of-plane displacement of the wall panel was prevented by a steel constraint (Figure 3a). The shear loading was induced with a servo-hydraulic actuator of capacity 160 kN fixed to the wall panel 15 cm above the floor panel. Teflon layer was inserted between the steel constraint and the wall panel to eliminate friction. Relative displacements between the wall and the floor panel were measured with four linear variable displacement transformers (LVDTs), positioned at ends of the wall on both sides.

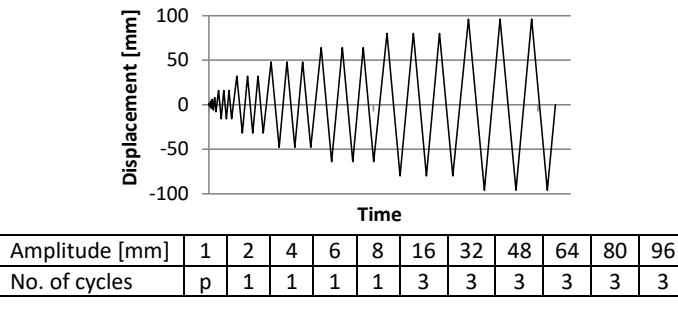
For both monotonic and cyclic tests the loading was induced by controlling the increase of lateral displacement; the rate of displacement was 0.2 mm/s. Cyclic loading was defined according to ISO 16670 (ISO, 2003). The amplitudes of the cyclic loading were determined based on the results of monotonic tests depending on the ultimate displacement  $d_{\text{u,max}}$ ; i.e. the displacement, at which the lateral resistance decreased to 80% of maximum capacity  $F_{\text{max}}$ . The induced lateral displacement time history is presented in Figure 3b.

Table 2. Testing program.

Test	Loading	Insulation type	<b>CLT Orientation</b>
Neiz/M	Monotonic	/	vertical
NF/M	Monotonic	NF	vertical
NB/M	Monotonic	NB	vertical
SR55/M	Monotonic	SR55	vertical
SR1200/M	Monotonic	SR1200	vertical
Neiz/Cs-1v	ISO	/	vertical
Neiz/Cs-1h	ISO	/	horizontal
SR1200/Cs-1h	ISO	SR1200	horizontal
SR1200/Cs-1v	ISO	SR1200	vertical
SR55/Cs-1h	ISO	SR55	horizontal
SR55/Cs-1v	ISO	SR55	vertical
NF/Cs-1v	ISO	NF	vertical
Nf/Cs-1h	ISO	NF	horizontal
NB/Cs-1h	ISO	NB	horizontal
NB/Cs-1v	ISO	NB	vertical



a.



b.

Figure 3. a. Test setup and b. Displacement time history.

## 3 ANALYSIS OF THE RESULTS

Seismic performance of the connections was evaluated by analyzing the force - displacement curves obtained in tests in correspondence to observed damage/failure mechanisms. Primarily, load-bearing and displacement capacities were determined, while more in-depth information of the behaviour of the connection and the influence of insulation bedding was obtained through analysis of the hysteresis curves obtained in cyclic tests.

## 3.1 Damage and failure mechanism

Both in monotonic and cyclic tests, the specimens exhibited ductile failure mechanism. Typical failure of specimens is presented in Figure 4a-d.

The results differed depending on the type of specimen. In case of specimens without insulation, embedding of screws (i.e. damage in wood around the screws) was followed by withdrawal from the wall panel (Figure 4a), while for specimens with insulation, a combination of withdrawal and shear failure of screws occurred. For both tests only minor withdrawal and uplift of the angle bracket from the floor panel were found. For specimens with insulation, embedding and withdrawal of the screws were in most cases more evident in the wall panel (Figure 4b), while in some cases withdrawal from floor panels was more evident (Figure 4c).

Shear failure of the screws in wall panel occurred in a few cases (Figure 4d). No major correlation between the type of insulation and the prevailing failure mechanism was found, except that withdrawal of screws from floor panel occurred usually with stiffer insulation (NF and SR1200) and that screws failed only in wall panels, where the grain orientation of the outer laminae was parallel to load direction (horizontal) and the specimens had either soft (NB, SR55) or no insulation.



a. Embedding and withdrawal of screws from the wall panel (uninsulated specimen)



b. Embedding and withdrawal of screws from the wall panel (insulated specimen)



c. Embedding and withdrawal of screws from the floor and wall panel (insulated specimen)



d. Embedding, withdrawal and shear failure of screws in the wall panel (insulated specimen)

Figure 4. Failure of different types of specimens and loading.

## 3.2 Load-bearing and displacement capacity

In Figure 5 force - displacement curves obtained in monotonic and cyclic tests for three types of specimens are presented; for specimen with no insulation (labelled "Neiz") and for the stiff and soft bedding insulations, "SR1200" and "SR55", respectively.

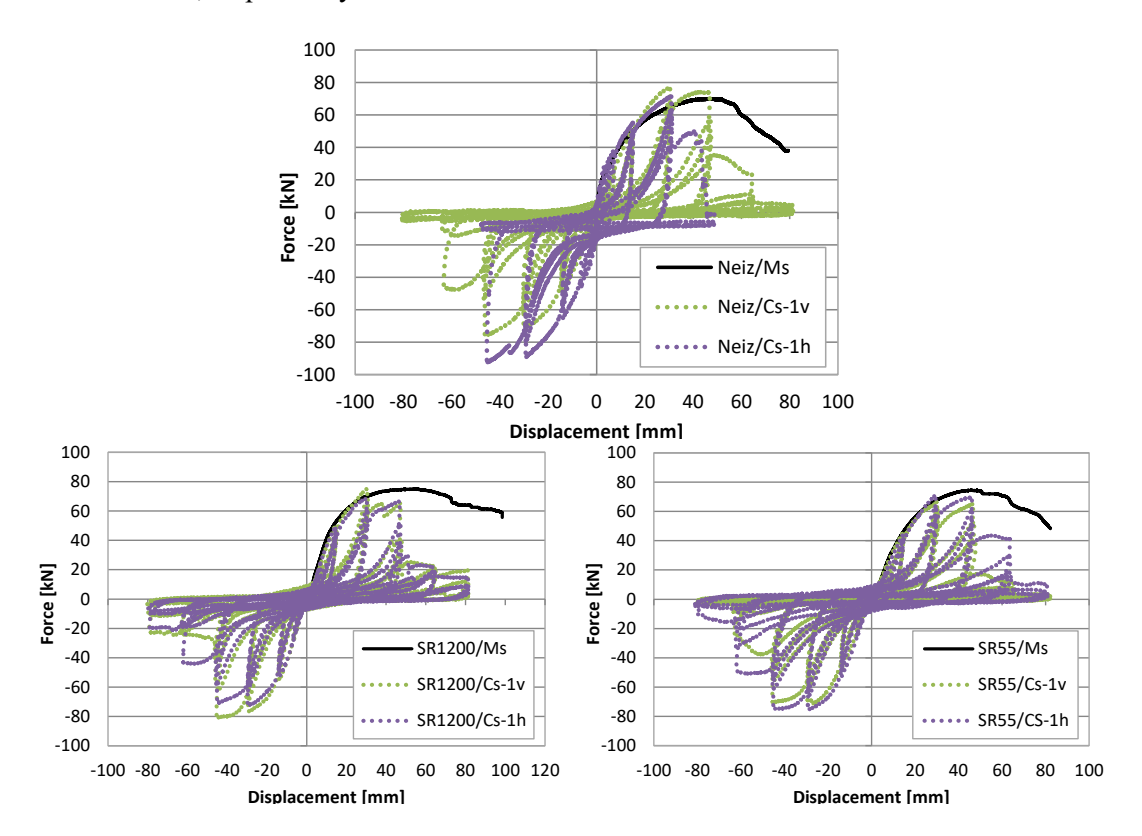


Figure 5. Lateral load displacement curves for three types of specimens; with no insulation (Neiz), with stiff bedding (SR1200) and with soft bedding (SR55) obtained in monotonic and cyclic tests.

For hysteresis curves of all specimens, pinching effect is evident. Pinching can be explained by the damage mechanism; with increasing of load and repeating of cycles, the screws damage the surrounding wood and create gaps. When the load is reversed, the screws move through the gaps and wood offers very small resistance.

As shown in Figure 5, there is no major difference in load capacity between specimens with different insulation bedding. Average maximum force obtained in cyclic tests for both directions of loading for all specimens was 75.7 kN, while for monotonic tests the average maximum force was 71.3 kN. It should be noted that the capacity of specimen NB/Ms was significantly lower than of other specimens; however the results of NB cyclic tests did not stand out (Figure 5). In all cases except in one case of cyclic loading the load resistance was higher in the negative direction (first direction of loading). While for most of the tests the difference of maximum resistance for the two directions of loading was under 5%, it was more than 20% in test Neiz/Cs-1h and more than 10% in test NB/Cs-1h. The maximum load-bearing capacity for both directions of loading ( $F_{\text{max}}$ ), corresponding displacements ( $d_{\text{Fmax}}$ ) and ultimate displacements corresponding to 80% post-peak load-bearing capacity ( $d_{\text{u,max}}$ ) for all tests are presented in Figure 6.

As shown in Figure 6, the ultimate displacement  $d_{u,max}$  was similar for all types of bedding; in cyclic tests,  $d_{u,max}$  was approximately 45 mm in both directions of loading. In monotonic tests,  $d_{u,max}$  was significantly larger (ranging from 49.3 to 95.7 mm with average value of 73.1 mm).

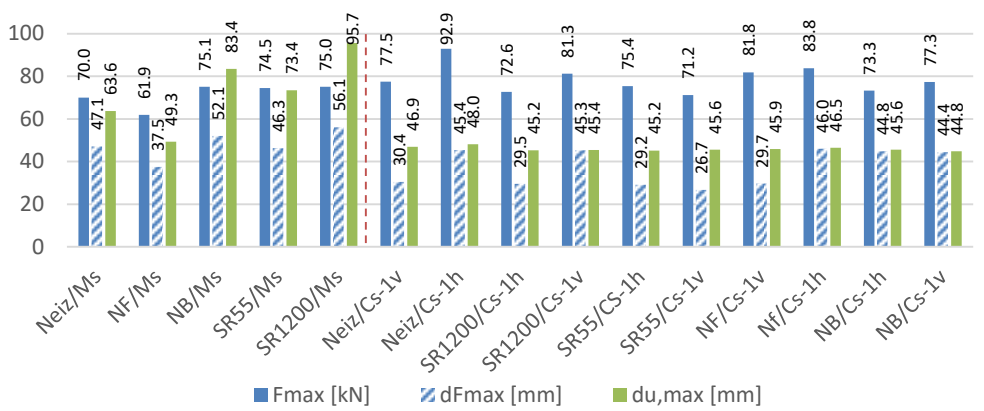


Figure 6. Performance of specimens (maximum resistance, corresponding displacement and ultimate displacement).

#### 3.3 Idealisation

To compare the behaviour in terms of ductility  $\mu$  (i.e. ratio of ultimate to yield displacement), the force - displacement diagrams were idealized to bi-linear curves according to Yasumura and Kawai (1998).

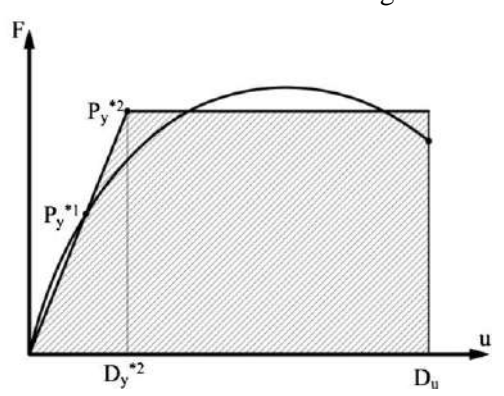


Figure 7. Determination of bi-linear curve according to Yasumura and Kawai (1998).

In Figure 8, a comparison of idealized shear capacity  $F_{id}$  and ductility  $\mu$  is presented. Average values from cyclic tests are compared to the results of monotonic tests.

Firstly, it was observed that the difference in shear resistance for different types of specimens was relatively small. The difference in ductility was larger, especially for monotonic tests – in general the uninsulated specimens exhibit larger ductility than insulated specimens although this did not apply to all cases (SR1200/Ms). The reason for this is higher stiffness of uninsulated specimens (as it is shown further in the paper), and consequently smaller yield displacement.

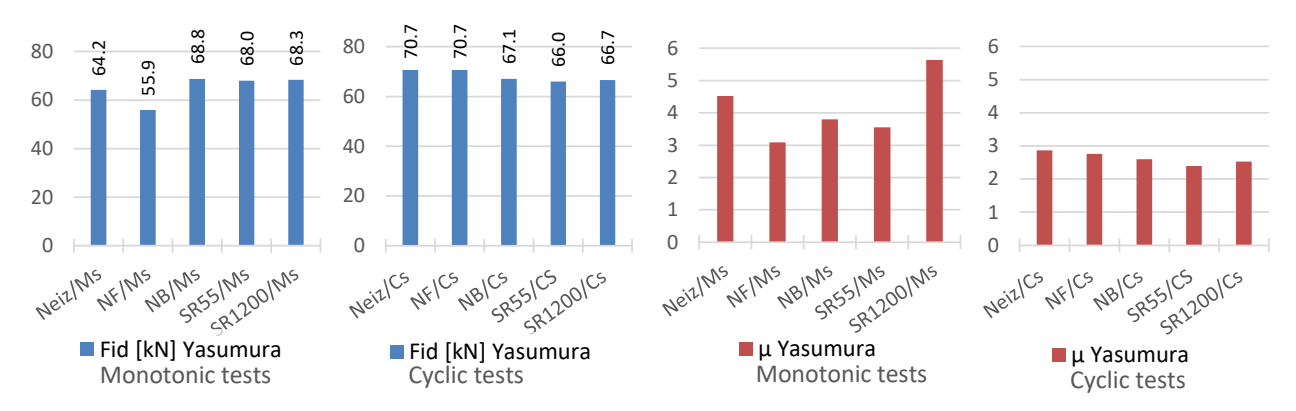


Figure 8. Idealized resistance  $F_{id}$  and ductility  $\mu$  according to Yasumura for monotonic tests and average value of both directions for cyclic tests with the same insulation type.

# 3.4 Stiffness comparison

While the insulation does not affect the load-bearing capacity, it reduces the stiffness, especially in the initial stages of loading (Figure 9). The initial stiffness (at 1 mm) of insulated specimens reaches in average only 30% of stiffness of uninsulated specimens at cyclic tests (29% at monotonic tests). In case of insulation bedding a considerable reduction of the effective stiffness  $K_{\text{eff}}$  (i.e. the stiffness of the idealized bi-linear curve according to Yasumura) is also obtained (Figure 10). For cyclic tests, the  $K_{\text{eff}}$  of insulated specimens ranges from 73% up to 87%  $K_{\text{eff}}$  of uninsulated specimens, while for monotonic from 69% to 88%.

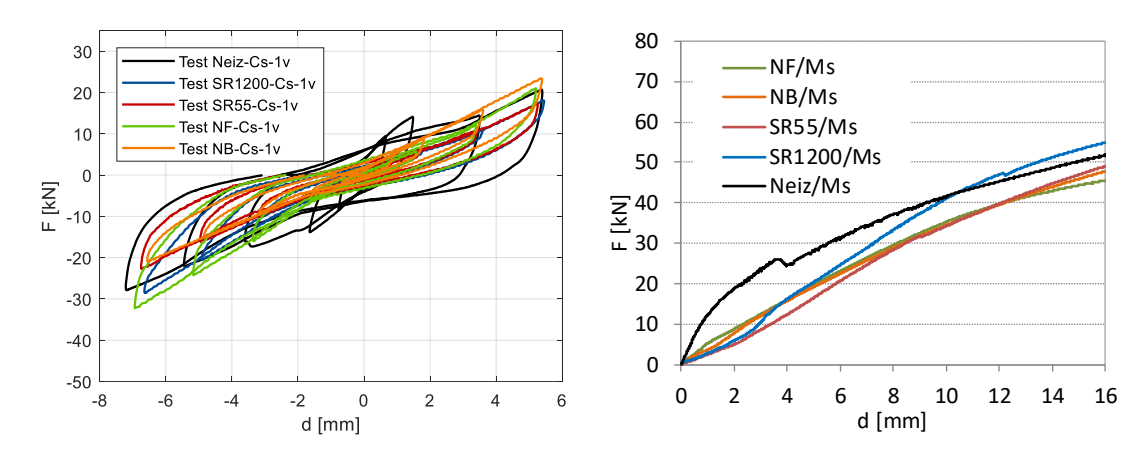


Figure 9. A comparison of first cycle hysteresis curves (left) and a comparison of monotonic curves (right) for different insulation specimens (outer CLT wall laminae vertical).

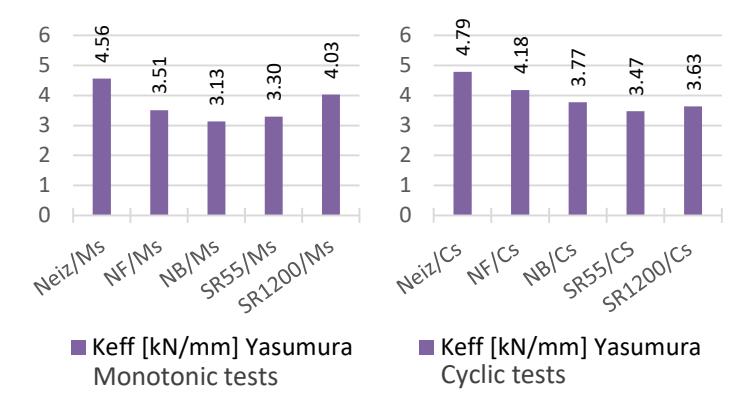


Figure 10. Comparison of effective stiffness of the bi-linear curve calculated according to Yasumura for monotonic tests and average value of both directions for cyclic tests with the same insulation type.

## 3.5 Energy dissipation and equivalent viscous damping

Energy dissipation and damping are evaluated from force - displacement hysteresis curves. Each cycle of loading, i.e. each loop, is analysed. The energy, dissipated at each loading cycle  $E_{\rm DIS}$ , is calculated as the area within one complete hysteresis loop (Figure 11a). In order to evaluate the relative amount of dissipation,  $E_{\rm DIS}$  is compared to input energy  $E_{\rm INP}$ , which is defined as the work of the actuator, needed to deform the connection up to a maximum amplitude displacement and presents the area under the positive and negative parts of the hysteresis loop (Figure 11a). Another parameter, which is more commonly used in the literature to evaluate dissipation, is equivalent viscous damping coefficient  $\xi$  (Chopra, 1995). It is defined according to Equation 1, where  $E_{\rm DIS}$  and  $E_{\rm INP}^{\ \ \ \ }$  are defined as in Figure 11b. In Figure 12 and Figure 13 a comparison of  $E_{\rm DIS}/E_{\rm INP}$  and of  $\xi$  is presented for uninsulated and insulated specimens with vertical orientation of CLT wall panel for first and for third cycles of loading.

$$\xi = \frac{E_{DIS}}{2\pi E_{INP}^*} \tag{1}$$

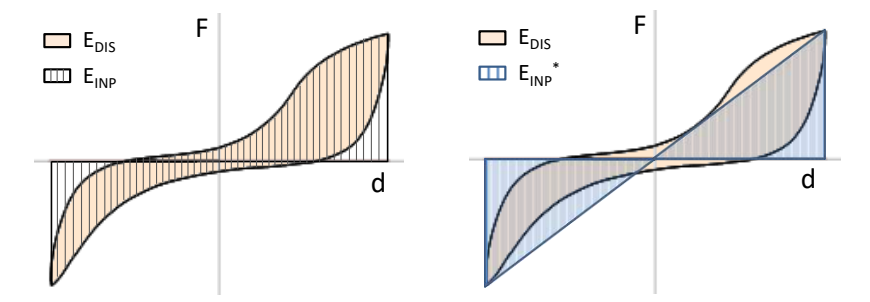


Figure 11. Dissipated energy  $E_{\text{DIS}}$  and input energy  $E_{\text{INP}}$  of one loading cycle (left) and dissipated and input energy  $E_{\text{INP}}^*$  for determining the equivalent damping coefficient  $\xi$  (right).

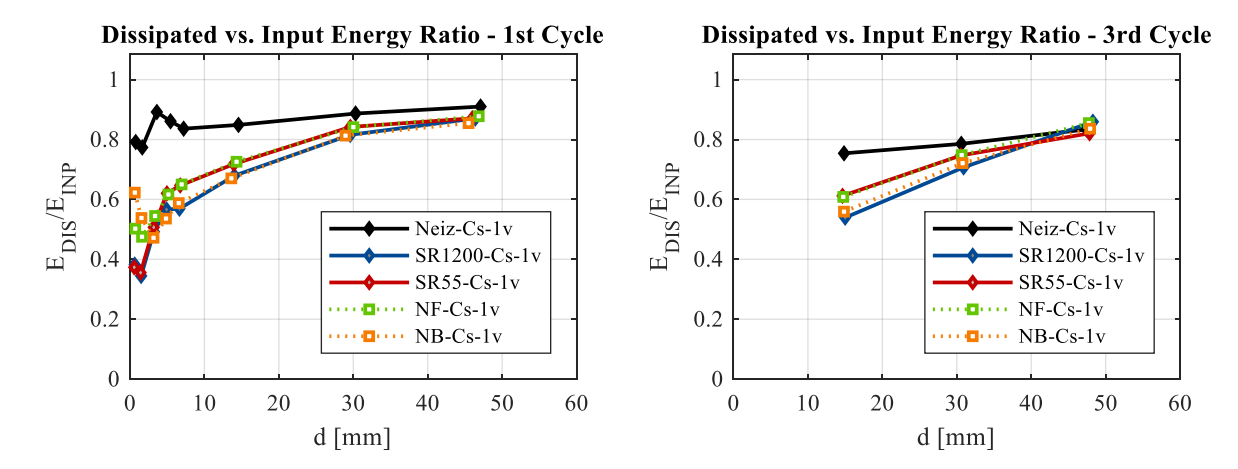


Figure 12. Ratio  $E_{\text{DIS}}/E_{\text{INP}}$  for tests with vertical outer CLT wall panel lamina obtained for the first cycle of loading (left) and for the third cycle of loading (right).

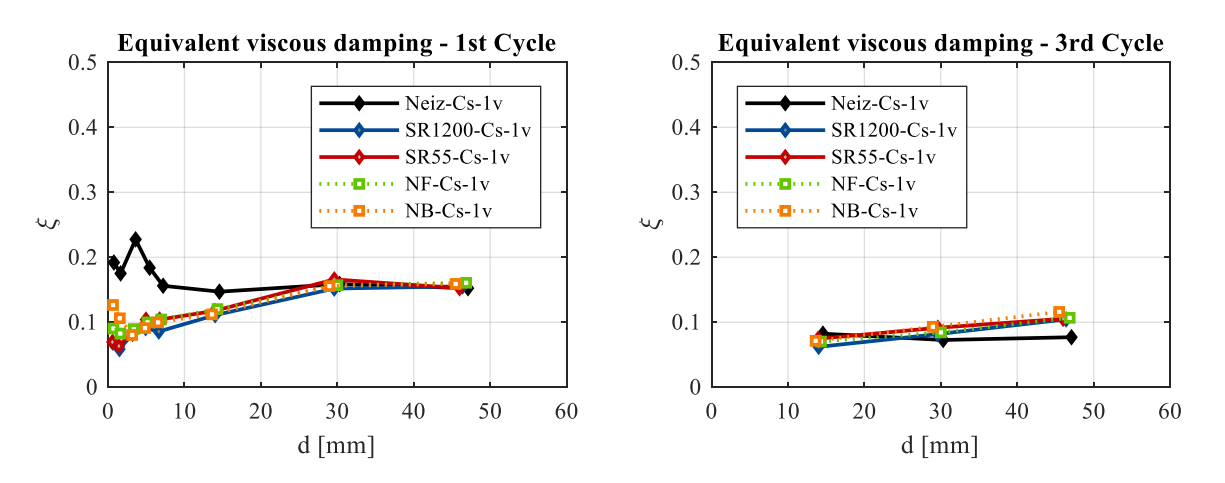


Figure 13. Equivalent damping coefficient  $\xi$  up to ultimate displacement for tests with vertical outer CLT wall panel lamina obtained for the first cycle of loading (left) and for the third cycle of loading (right).

Figures 12 and 13 show that uninsulated specimens exhibit larger energy dissipation and viscous damping than insulated specimens. The difference is the largest in the initial cycles of loading and is decreasing with the amplitude of the displacement. At the displacement corresponding to maximum resistance (approx. at 30 mm) there is almost no difference between the insulated and uninsulated specimens. Values for  $\xi$  range for the first cycle between 0.11 and 0.23 for uninsulated and between 0.05 and 0.24 for insulated specimens. Values for  $E_{\text{DIS}}/E_{\text{INP}}$  range for the first cycle between 0.54 and 0.99 for uninsulated and between 0.30 and 0.99 for the insulated system.

#### 4 CONCLUSIONS

An experimental campaign including monotonic and cyclic shear tests of innovative insulated CLT steel angle bracket connections was conducted to study the seismic behaviour of the connections and furthermore to determine the influence of the insulation bedding between CLT panels.

From the study, the following conclusions can be made:

- The innovative connection enables ductile shear response. In all cases, the failure occurred due to the large deformations of screws in the wall panels. The inclined screws which enable the connection between the angle brackets and the floor panels were not critical and no brittle failures of brackets or other connection components were observed during the tests.
- The comparison of response of the connection system with and without the insulation bedding proved that none of the tested insulation bedding significantly influences the load-bearing and displacement capacity of the system. Average shear resistance of the system without bedding obtained for cyclic tests was 79.6 kN, while it ranged from 71.1 to 80.7 kN for systems with insulation. Average ultimate displacements obtained in cyclic tests equaled approximately 45 mm for all types of insulation.
- While the insulation bedding does not have much influence on the load-bearing capacity and the ductility of the system, it changes significantly the stiffness characteristics; The insulation bedding reduces the effective stiffness in average by 21% for cyclic tests, whereas initial stiffness (evaluated at 1 mm) in average by 71%.
- The difference in stiffness is the largest at small displacements. Therefore, the differences in rigidity need to be considered when designing the structure for the serviceability limit states.
- Relative energy dissipation and equivalent viscous damping are in general lower in case of insulated systems than in the case of uninsulated systems. The difference however decreases with increasing displacements. Therefore no major differences are expected in case of severe seismic loading.

In this paper, the behaviour of insulated connection between CLT panels under pure shear loading was investigated. In the next stage of the research, the behaviour of the connection in the vertical direction (uplift) and under a combination of vertical and shear loads will be tested. This will enable a more comprehensive understanding of the behaviour of the connection during seismic loads.

## 5 ACKNOWLEDGMENTS

The authors acknowledge European Commission for funding the InnoRenew CoE project under the Horizon2020 Widespread-Teaming program [Grant Agreement #739574] and companies Getzner and Pitzl.

## 6 REFERENCES

Abrahamsen R., AS M.L. (2017). Mjøstårnet-Construction of an 81 m tall timber building, in: International House Forum.

Azinović B., Kramar M., Pazlar T., Kwiecien A., Weckendorf J., Šušteršič I., (2018). Experimental and Numerical Analysis of Flexible Polymer Connections for CLT Buildings, in: *Proceedings WCTE 2018*. Seoul, South Korea.

Benedetti F., Rosales V., Opazo A. (2016). Cyclic testing and simulation of hold-down connections in radiata pine CLT shear walls, in: *Proceedings WCTE 2016*. Vienna, Austria.

Casagrande D., Polastri A., Sartori T., Loss C., Chiodega M. (2016). Experimental tests for mechanical characterization of timber buildings connections, in: *Proceedings WCTE 2016*. Vienna, Austria.

CEN. (2005). EN12512:2005 Timber structures - Test methods - Cyclic testing of joints made with mechanical fasteners.

Chopra A.K. (1995). Dynamics of Structures.

D'Arenzo G., Rinaldin G., Fossetti M., Fragiacomo M., Nebiolo F., Chiodega M. (2018) Tensile and shear behaviour of an innovative angle bracket for CLT structures, in: *Proceedings WCTE 2018*. Seoul, South Korea.

Flatscher G., Bratulić K., Schickhofer G. (2015) Experimental tests on cross-laminated timber joints and walls. *Proceedings of the ICE - Structures and Buildings* (168): 868–877.

Fragiacomo M., Dujič B., Šušteršič I. (2011) Elastic and ductile design of multi-storey crosslam massive wooden buildings under seismic actions. *Engineering structures* (33): 3043–3053.

Gavrić I., Fragiacomo M., Ceccotti A. (2015) Cyclic behaviour of typical metal connectors for cross-laminated (CLT) structures. *Materials and Structures* (48): 1841–1857.

Getzner, (2018) Intelligent sound insulation solutions in wood construction. Getzner Werkstoffe. URL https://www.getzner.com/en/applications/construction/building-acoustics/resilient-bedding-of-elements-in-timber-construction (accessed 2.1.2019).

ISO. (2003) ISO 16670:2003 Timber structures - Joints made with mechanical fasteners - Quasi-static reversed-cyclic test method. International Organization for Standardization.

Liu, J., Lam, F., 2018. Experimental test of coupling effect on CLT angle bracket connections. Engineering Structures 171, 862–873. https://doi.org/10.1016/j.engstruct.2018.05.013

Pei S., van de Lindt J.W. (2011) Seismic numerical modeling of a six-story light-frame wood building: Comparison with experiments. *Journal of Earthquake Engineering* (15): 924–941.

Pitzl, Getzner, (2018) GePi connectors: Powerful soundproofing angle brackets. URL https://www.pitzl-connectors.com/gepi/ (accessed 2.1.2019).

Reynolds T., Harris R., Chang W.-S., Bregulla J., Bawcombe J. (2015) Ambient vibration tests of a cross-laminated timber building. *Proceedings of the ICE - Construction Materials* (168): 121–131.

Tomasi R., Smith I. (2015) Experimental Characterization of Monotonic and Cyclic Loading Responses of CLT Panel-To-Foundation Angle Bracket Connections. *Journal of Materials in Civil Engineering* (27).

Yasumura M., Kawai N. (1998). Estimating seismic performance of wood-framed structures, in: *Proceedings of 5th WCTE*.